EIGHTEENTH EUROPEAN ROTORCRAFT FORUM

B - 09

Paper No. 19

Unsteady Lift of an Airfoil with a Trailing-Edge Flap based on Indicial Concepts

J. Gordon Leishman
Department of Aerospace Engineering,
University of Maryland,
College Park, Maryland, USA

September 15-18, 1992

AVIGNON, FRANCE

ASSOCIATION AERONAUTIQUE ET ASTRONAUTIQUE DE FRANCE

Unsteady Lift of an Airfoil with a Trailing–Edge Flap based on Indicial Concepts

J. Gordon Leishman*

Department of Aerospace Engineering
University of Maryland at College Park, Maryland 20742, USA.

ABSTRACT - A practical method is described for computing the unsteady lift on an airfoil due to arbitrary motion of a trailing–edge flap. The result for the incompressible case is obtained in state-space (differential equation) form by means of Duhamel superposition and employing an exponential approximation to Wagner's indicial lift function. For subsonic compressible flow, the indicial lift at small values of time due to impulsive trailing–edge flap deflection is obtained from linear theory in conjunction with the aerodynamic reciprocal theorems. These exact results are used to help obtain complete exponential approximations for the indicial response due to impulsive flap deflection. The final result for the unsteady lift due to an arbitrary flap deflection in subsonic flow is obtained in state-space form. Numerical results are shown illustrating the overall significance of both unsteady effects and compressibility effects on airfoils with unsteady trailing–edge flap motions in a simulated helicopter rotor environment. The effects of Mach number on the aerodynamic response were shown to be especially significant, and essentially manifest themselves as larger aerodynamic lags at higher Mach numbers.

NOMENCLATURE

a	Pitch axis location (semi–chords)	S	Distance traveled in semi–chords, $2Vt/c$
a_s	Sonic velocity	t	Time
A_i	Coefficients of indicial functions	t_1	Non-dimensional time
b	Semichord, $c/2$	T_i	Basic noncirculatory time constant, c/a_s
b_i	Exponents of indicial functions	V	Free-stream velocity
c	Airfoil chord	w_g	Gust upwash velocity
$C(k)$	Theodorsen's function	x	Airfoil chord axis, origin at mid–chord
C_L	Lift force coefficient	z_i	State variable
C_p	Pressure coefficient	α	Angle of attack
e	Flap hinge location (semi–chords)	β	Compressibility factor, $\sqrt{1-M^2}$
F_1, F_4, F_{10}, F_{11}	Geometric constants for flap	δ	Flap deflection angle
h	Plunge displacement, positive downward	Δ	Incremental quantity
k	Reduced frequency, $\omega c/2V$	ρ	Fluid density
K	Non-circulatory time constant	ϕ	Indicial response function
M	Mach number	ϕ_W, ψ	Wagner and Künsser functions, respectively
q	Non-dimensional pitch rate, $\dot{\alpha}c/V$	ω	Frequency

Subscripts and Superscripts

$(.)_q$	Refers to airfoil pitch rate	$(.)^c$	Refers to circulatory component
$(.)_\alpha$	Refers to angle of attack	$(.)^i$	Refers to noncirculatory (impulsive) component
$(.)_\delta$	Refers to flap deflection angle	$(.)^f$	Refers to flap component
$(.)_{\dot{\delta}}$	Refers to flap deflection rate about hinge		

INTRODUCTION

There have been several practical applications of a trailing–edge flap for gust alleviation or to help suppress flutter on fixed-wing aircraft, e.g., [1]. For helicopter rotors the use of trailing–edge flaps on the blades has, so far at least, found use only for 1/rev. cyclic pitch control, e.g., the Kaman servo–flap. However, with the advent

*Assistant Professor.

Presented as paper No.19, Eighteenth European Rotorcraft Forum, Avignon, France, Sept. 15-18, 1992.

of smart materials/structures and high bandwidth active control technologies, it is now becoming increasingly feasible to use compliant airfoil surfaces or trailing–edge mounted flaps on rotor blades as a means of individual blade control (IBC). Coupled with real–time adaptive feedback strategies, actively controlling the blade lift distribution offers tremendous possibilities for improving helicopter rotor performance, as well as reducing blade loads and vibrations [2]. Potentially, there are several other benefits to be gained by actively optimizing blade lift. These include improved forward flight performance by the active suppression of blade stall, reducing advancing blade transonic drag, reduced rotor noise by alleviating the intensity of blade/wake or blade/tip vortex interaction phenomena, and possibly improving the aircraft flight dynamics and maneuverability.

A practical concern of IBC, is the availability of suitable low mass high force actuators that can be mounted inside the rotating blade and used to drive the compliant aerodynamic surfaces at relatively high frequencies. Initial results from smart structures and materials research at the University of Maryland, has shown that IBC is possible on a Froude-scale rotor by means of a small outboard trailing–edge flap controlled by piezoceramic actuators [3]. Some objectives of this program are to use a smart-structures based IBC concept to explore methods of reducing rotor vibration, optimize rotor performance, and to improve the acoustic signature, especially in descents where strong interactions with discrete tip vortices produce a form of impulsive rotor noise known as blade slap.

Parallel theoretical studies of these problems using advanced rotor models require the use of a suitable time–domain aerodynamic theory for the flap. An unsteady aerodynamic theory is required for the problem, firstly because the flap actuation frequency could be many times the rotor rotational frequency, and secondly because high resolution acoustic predictions of overall rotor noise need be made. In addition, since the local effective reduced frequencies based on flap motion often exceed unity on an IBC rotor, incompressible assumptions are no longer adequate and compressible flow must be intrinsically assumed. Until now, there has been no available unsteady aerodynamic theory (in the form required for rotor calculations) for the effects of trailing–edge flap motions. The objective of this article is to describe the development of such a theory based on indicial function concepts, and to present some illustrative results showing the general significance of unsteady effects associated with time–varying trailing–edge flap displacements in a simulated rotor environment.

METHODOLOGY

The problem described herein is formulated in the spirit of classical unsteady airfoil theory. The assumptions are basically that the unsteady problem is governed by the linearized partial differential equation and linearized boundary conditions. We will assume constant flow velocity, although the results can be extended to time–varying free–streams and the procedures are outlined for incompressible flow in [4]. For conciseness in this article, we will address only the lift response, although results for the pitching moment have also been derived. As a precursor, the solution for the unsteady lift in the time–domain due to arbitrary flap motion in incompressible flow is obtained, followed by a solution for the subsonic compressible case.

Incompressible Flow

The unsteady lift on an airfoil with a harmonically oscillating flap in incompressible flow has been examined by Küssner and Schwarz [5] and others, but the most well known solution is that due to Theodorsen [6, 7]. The lift on a thin rigid airfoil undergoing oscillatory forcing in an incompressible flow of steady velocity V, and comprising non–steady displacements in plunge (h), angle of attack (α), and pitch rate ($\dot{\alpha}$) about some pitch axis a distance a semi-chords from the airfoil mid-chord axis (see Fig. 1) can be written in coefficient form as

$$C_L = \frac{\pi b}{V^2}\left[\ddot{h} + V\dot{\alpha} - ba\ddot{\alpha}\right] + 2\pi C(k)\left[\frac{\dot{h}}{V} + \alpha + b\left(\frac{1}{2} - a\right)\frac{\dot{\alpha}}{V}\right] \tag{1}$$

The first group of terms are the noncirculatory or apparent mass components and account for the inertia of the fluid. The second group of terms are the circulatory components, where $C(k)$ is the well known Theodorsen function and accounts for the influence of the shed wake vorticity.

With the addition of a trailing-edge flap with hinge at a distance eb from the mid-chord, there are additional airloads that depend on the flap deflection angle, δ, and its time rate–of–change, $\dot{\delta}$. The additional lift coefficient is

$$C_L^f = \frac{b}{V}\left[-VF_4\dot{\delta} - bF_1\ddot{\delta}\right] + 2\pi C(k)\left[\frac{F_{10}\delta}{\pi} + \frac{bF_{11}\dot{\delta}}{2\pi V}\right] \tag{2}$$

where again, the first and second group of terms are the noncirculatory and circulatory loads, respectively. The coefficients F_1, F_4, F_{10} and F_{11} are all geometric terms, which depend only on the size of the flap relative to the airfoil chord and for a coordinate system located at mid–chord can be expressed as

$$\begin{aligned} F_1 &= e\cos^{-1}e - \tfrac{1}{3}(2+e^2)\sqrt{1-e^2} \quad & F_4 &= e\sqrt{1-e^2} - \cos^{-1}e \\ F_{10} &= \sqrt{1-e^2} + \cos^{-1}e & F_{11} &= (1-2e)\cos^{-1}e + (2-e)\sqrt{1-e^2} \end{aligned} \tag{3}$$

Finally, we can write

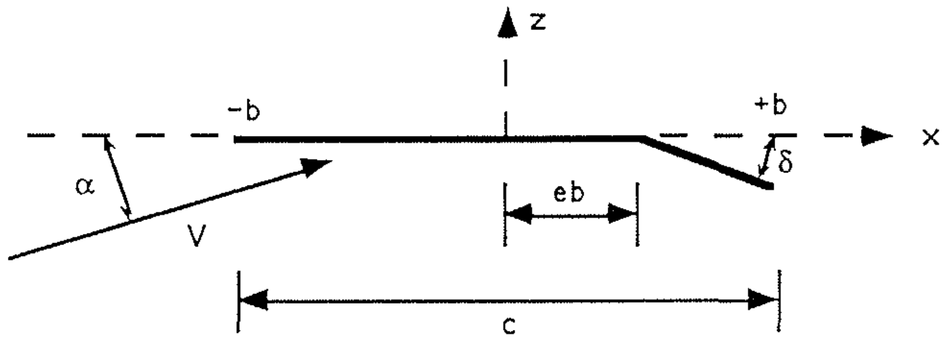

Figure 1: Nomenclature for airfoil and flap

$$C_L(t) = \frac{\pi b}{V^2}\left[\ddot{h} + V\dot{\alpha} - ba\ddot{\alpha}\right] + \frac{b}{V}\left[-VF_4\dot{\delta} - bF_1\ddot{\delta}\right] + 2\pi C(k)\left[\alpha_{qs} + \delta_{qs}\right] \tag{4}$$

where α_{qs} is the quasi-steady airfoil angle of attack, and δ_{qs} is the quasi-steady angle of attack due to the imposed flap deflection, i.e.,

$$\alpha_{qs} = \left[\frac{\dot{h}}{V} + \alpha + b\left(\frac{1}{2} - a\right)\frac{\dot{\alpha}}{V}\right] \qquad \delta_{qs} = \left[\frac{F_{10}\delta}{\pi} + \frac{bF_{11}\dot{\delta}}{2\pi V}\right] = \left[\frac{F_{10}\delta}{\pi} + \frac{F_{11}\dot{\delta}c}{4\pi V}\right] \tag{5}$$

Eq. 4 holds only for harmonic motion of the airfoil and/or the flap.

For the case of arbitrary airfoil motion and/or arbitrary flap deflection in a steady flow of velocity V, the result for the unsteady lift can be obtained by means of Duhamel's superposition integral with the Wagner indicial (step) response, and can be written as

$$\begin{aligned} C_L(t) &= \frac{\pi b}{V^2}\left[\ddot{h} + V\dot{\alpha} - ba\ddot{\alpha}\right] + \frac{b}{V}\left[-VF_4\dot{\delta} - bF_1\ddot{\delta}\right] \\ &\quad + 2\pi\left[\alpha_{qs}(0)\phi_W(S) + \int_0^S \frac{d\alpha_{qs}}{d\sigma}\phi_W(S-\sigma)d\sigma + \delta_{qs}(0)\phi_W(S) + \int_0^S \frac{d\delta_{qs}}{d\sigma}\phi_W(S-\sigma)d\sigma\right] \end{aligned} \tag{6}$$

where ϕ_W is the Wagner function, and S $(= Vt/b)$ is the aerodynamic time based on semi-chord lengths of airfoil travel. The Wagner function accounts for the influence of the shed wake, and is known exactly in terms of Bessel functions [8, 9, 10]. In fact, the Theodorsen function and the Wagner function are related by means of a Fourier transform pair. For practical evaluation of the Duhamel integral, the Wagner function can be expressed as an exponential approximation. Consider a second order indicial response approximation, i.e.,

$$\phi_W(S) = 1 - A_1\exp(-b_1 S) - A_2\exp(-b_2 S) \tag{7}$$

where $A_1 + A_2 = 0.5$. A non-linear least squares fit to the Wagner result using a constrained optimization algorithm gives $A_1 = 0.2048, A_2 = 0.2952, b_1 = 0.0557$ and $b_2 = 0.333$, with an error of less than 0.1% of the exact solution. Other fits to the Wagner function are given by R.T. Jones [11], W.P. Jones [12] and others [13, 14]. In the t (real time) domain we can write the indicial response as

$$\phi_W(t) = 1 - A_1\exp(-t/T_1) - A_2\exp(-t/T_2) \tag{8}$$

where $T_1 = b/Vb_1$, $T_2 = b/Vb_2$. The Laplace transform of the corresponding impulse response can be written as a ratio of polynomials as

$$h(p) = \frac{(A_1 b_1 + A_2 b_2)(V/b)p + b_1 b_2 (V/b)^2}{p^2 + (b_1 + b_2)(V/b)p + b_1 b_2 (V/b)^2} \tag{9}$$

From this form, the state-space equivalent of the Duhamel integral

$$\alpha_{qs}(0)\phi_W(S) + \int_0^S \frac{d\alpha_{qs}}{d\sigma}\phi_W(S-\sigma)d\sigma \tag{10}$$

can be written in controllable canonical form as

$$\begin{bmatrix} \dot{z}_1(t) \\ \dot{z}_2(t) \end{bmatrix} = \begin{bmatrix} 0 & 1 \\ -b_1 b_2 (V/b)^2 & -(b_1 + b_2)(V/b) \end{bmatrix} \begin{bmatrix} z_1(t) \\ z_2(t) \end{bmatrix} + \begin{bmatrix} 0 \\ 1 \end{bmatrix} \alpha_{qs}(t) \tag{11}$$

and the output equation for the circulatory part of the lift coefficient due to arbitrary airfoil motion is

$$C^c_{L_\alpha}(t) = 2\pi \left[\begin{array}{cc} (b_1 b_2/2)(V/b)^2 & (A_1 b_1 + A_2 b_2)(V/b) \end{array} \right] \left[\begin{array}{c} z_1(t) \\ z_2(t) \end{array} \right] + \pi\alpha_{qs}(t) \tag{12}$$

Note that the second term on the right hand side arises because of the non-zero initial conditions of the Wagner function, i.e., $A_1 + A_2 = 0.5$. These first order differential equations are in the form $\dot{\mathbf{z}} = \mathbf{Az} + \mathbf{Bu}$ with the output equations $\mathbf{y} = \mathbf{Cz} + \mathbf{Du}$, where $\dot{z} = dz/dt$; $\mathbf{u} = u_i$, $i = 1, 2, ..., m$ are forcing function(s), and the $\mathbf{y} = y_i$, $i = 1, 2, ..., p$ are the airloads. $\mathbf{z} = z_i$, $i = 1, 2, ..., n$ are the states of the system. The states contain all the hereditary information about the aerodynamic system.

Similarly, if we consider the arbitrary trailing-edge flap motion, the state-space equivalent of

$$\delta_{qs}(0)\phi_W(S) + \int_0^S \frac{d\delta_{qs}}{d\sigma}\phi_W(S-\sigma)d\sigma \tag{13}$$

can be written as

$$\left[\begin{array}{c} \dot{z}_3(t) \\ \dot{z}_4(t) \end{array} \right] = \left[\begin{array}{cc} 0 & 1 \\ -b_1 b_2 (V/b)^2 & -(b_1 + b_2)(V/b) \end{array} \right] \left[\begin{array}{c} z_3(t) \\ z_4(t) \end{array} \right] + \left[\begin{array}{c} 0 \\ 1 \end{array} \right] \delta_{qs}(t) \tag{14}$$

and the output equation for the circulatory part of the lift coefficient due to arbitrary flap motion is

$$C^c_{L_\delta}(t) = 2\pi \left[\begin{array}{cc} (b_1 b_2/2)(V/c)^2 & (A_1 b_1 + A_2 b_2)(V/b) \end{array} \right] \left[\begin{array}{c} z_3(t) \\ z_4(t) \end{array} \right] + \pi\delta_{qs}(t) \tag{15}$$

Note that the the $\mathbf{A}$ and $\mathbf{C}$ matrices are the same as for the angle of attack terms. This is because the circulatory lift lag is an intrinsic function of the fluid and does not depend on the airfoil boundary conditions. In all cases, the chordwise pressure variation due to the shed wake vorticity is still the same as the thin airfoil loading, and is unaffected by the mode of forcing, pitch axis location or flap deflection. In other words, the circulatory part of the indicial response is the same for all modes of forcing.

The noncirculatory parts of the lift, which for an incompressible flow are proportional to the instantaneous displacements and involve no states, can be written as

$$C^i_L(t) = \frac{\pi b}{V}\left[\ddot{h} + V\dot{\alpha} - ba\ddot{\alpha}\right] + \frac{b}{V^2}\left[-VF_4\dot{\delta} - bF_1\ddot{\delta}\right] \tag{16}$$

Therefore, the total lift due to independent arbitrary airfoil motion and flap deflection can be written as

$$C^c_L(t) = C^c_{L_\alpha}(t) + C^c_{L_\delta}(t) + C^i_L(t) \tag{17}$$

In addition to the foregoing the airfoil operates in an arbitrary gust field, and it is important to consider this part of the lift response. Denoting the the downwash velocity by w_g, the unsteady lift in the time domain can be found by using Duhamel superposition with the Küssner gust entry function, $\psi(S)$, i.e.,

$$C^g_L(t) = 2\pi\left[\frac{w_g(0)}{V}\psi(S) + \frac{1}{V}\int_0^S \frac{dw_g}{d\sigma}\psi(S-\sigma)d\sigma\right] \tag{18}$$

Like the Wagner function, the Küssner gust entry function is also known exactly in terms of Bessel functions [10]. However, for practical calculations it is convenient to approximate the Küssner function using

$$\psi(S) = 1 - A_3\exp(-b_3 S) - A_4\exp(-b_4 S) \tag{19}$$

where $A_3 + A_4 = 1$. A non-linear least squares fit to Küssners' exact result can be made using a constrained optimization giving $A_3 = 0.5792, A_4 = 0.4208, b_3 = 0.1393$ and $b_4 = 1.802$, with an error of less than 0.1%. In state-space form, we can write Eq. 18 as

$$\left[\begin{array}{c} \dot{z}_5(t) \\ \dot{z}_6(t) \end{array} \right] = \left[\begin{array}{cc} 0 & 1 \\ -b_3 b_4 (V/b)^2 & -(b_3 + b_4)(V/b) \end{array} \right] \left[\begin{array}{c} z_5(t) \\ z_6(t) \end{array} \right] + \left[\begin{array}{c} 0 \\ 1 \end{array} \right] \frac{w_g(t)}{V} \tag{20}$$

and the output equation for the total lift coefficient due to the gust field is

$$C^g_L(t) = 2\pi \left[\begin{array}{cc} (b_3 b_4)(V/b)^2 & (A_3 b_3 + A_4 b_4)(V/b) \end{array} \right] \left[\begin{array}{c} z_5(t) \\ z_6(t) \end{array} \right] \tag{21}$$

The complete aerodynamic system for the airfoil in an incompressible flow, therefore, consists of 6 aerodynamic states. Although it is convenient for the present exposition to separate out the circulatory lift due to airfoil motion from that due to the flap motion, in a practical application their net effects can be combined so that only 2 states are required for the circulatory loads instead of four. The resulting four state equations describing the lift for arbitrary airfoil motion and flap motion (two states), and the gust field (two states) can be integrated in time using any standard ODE solver. Also, note that on a thin airfoil in an incompressible flow the circulatory lift always acts at the 1/4-chord point, and there are no additional states required for the moment. In the real case however, the aerodynamic center x_{ac} is not located at the 1/4–chord so that the pitching moment about the 1/4–chord must be be obtained from

$$C_M = (C_L^c + C_L^q)\left(\frac{1}{4} - x_{ac}\right) + \text{non-circulatory terms} \tag{22}$$

Compressible Flow

There are no equivalent exact results analogous to Theodorsen's theory for the unsteady lift due to airfoil or flap motion in subsonic compressible flow. For the subsonic oscillatory case, the flow is governed by the Poisso integral equation for which there is no known exact analytical solution. However, some numerical solutions for an oscillating flap have been computed by Turner and Rebinowitz [15].

Basically, in a compressible flow both the circulatory and the noncirculatory loads have a hereditary effect, and the latter are no longer proportional to the instantaneous displacements as in the incompressible case. We still seek a solution starting from the indicial response, since it has been shown previously that this permits a generalization to arbitrary forcing by means of Duhamel superposition. However, while the initial ($S = 0$) and final ($S = \infty$) values of the indicial response are known exactly in subsonic flow, the intermediate behavior is known exactly only for very limited values of time. Also, it is known that no simple compressibility scaling applies to the incompressible indicial result, i.e., it is not possible of to scale the Wagner indicial result as a function of Mach number.

The initial airloading on an airfoil operating in a compressible flow in response to a step change in the boundary conditions is associated with the acoustic wave system created by the initial perturbation. The airloading at $S = 0$ can be computed directly using piston theory. For indicial airfoil motion due to angle of attack and pitch rate about an axis a semi–chords downstream from mid–chord we obtain

$$\Delta C_{L_\alpha}(S=0,M) = \frac{4}{M}\Delta\alpha \quad \text{and} \quad \Delta C_{L_q}(S=0,M,a) = -\frac{2a}{M}\Delta q \tag{23}$$

and for indicial flap motion about a hinge point located e semi–chords downstream of mid–chord

$$\Delta C_{L_\delta}(S=0,M) = \frac{2(1-e)}{M}\Delta\delta \quad \text{and} \quad \Delta C_{L_{\dot\delta}}(S=0,M) = \frac{(1-e)^2}{2M}\frac{\Delta\dot\delta c}{V} \tag{24}$$

Note that these results are valid for any Mach number M, pitch axis location a, and flap hinge e, but only at the instant in time when the perturbation is applied. The final values of the indicial response are given by the usual linearized steady state (circulatory) theory, so that for indicial airfoil motion

$$\Delta C_{L_\alpha}(S=\infty,M) = \frac{2\pi}{\beta}\Delta\alpha \quad \text{and} \quad \Delta C_{L_q}(S=\infty,M,a) = \frac{2\pi}{\beta}\left(\frac{1}{2} - a\right)\Delta q \tag{25}$$

and for indicial flap motion

$$\Delta C_{L_\delta}(S=\infty,M) = \frac{2F_{10}}{\beta}\Delta\delta \quad \text{and} \quad \Delta C_{L_{\dot\delta}}(S=\infty,M) = \frac{F_{11}}{2\beta}\frac{\Delta\dot\delta c}{V} \tag{26}$$

The problem now is to define the intermediate behavior between $S =$ and $S = \infty$. The indicial lift coefficients due to angle of attack α and pitch rate q (about some reference axis a) can be conveniently subdivided into a sum of noncirculatory and circulatory parts. They can be approximated by the general equations

$$\Delta C_{L_\alpha}(S,M) = \left[\frac{4}{M}\phi_\alpha^i(S,M) + \frac{2\pi}{\beta}\phi_\alpha^c(S,M)\right]\Delta\alpha \tag{27}$$

$$\Delta C_{L_q}(S,M,a) = \left[-\frac{2a}{M}\phi_q^i(S,M,a) + \frac{2\pi}{\beta}\left(\frac{1}{2} - a\right)\phi_q^c(S,M,a)\right]\Delta q \tag{28}$$

Similarly, the indicial lift coefficients due to impulsive flap deflection (about some axis e) can be written as

$$\Delta C_{L_\delta}(S,M,e) = \left[\frac{2(1-e)}{M}\phi_\delta^i(S,M,e) + \frac{2F_{10}}{\beta}\phi_\delta^c(S,M,e)\right]\Delta\delta \tag{29}$$

$$\Delta C_{L_{\dot\delta}}(S,M,e) = \left[\frac{(1-e)^2}{2M}\phi_{\dot\delta}^i(S,M,e) + \frac{F_{11}}{2\beta}\phi_{\dot\delta}^c(S,M,e)\right]\frac{\Delta\dot\delta c}{V} \tag{30}$$

where the indicial response functions ϕ_α^c, ϕ_q^c, ϕ_α^i, ϕ_q^i, ϕ_δ^c, $\phi_{\dot\delta}^c$, ϕ_δ^i, and $\phi_{\dot\delta}^i$ all represent the intermediate behavior of the respective indicial airloads between $S = 0$ and $S = \infty$.

The circulatory part of the indicial response accounts for the influence of the shed wake vorticity. For a subsonic flow, it can be shown that the circulatory part of the indicial response due to changes in angle of attack, ϕ_α^c, can be approximated by the exponential function

$$\phi_\alpha^c(S,M) = 1 - \sum_{i=1}^{N} A_i \exp(-b_i \beta^2 S) \tag{31}$$

The poles of this function scale with β^2, which has been previously justified from experiments [16, 17] and is simply a manifestation of the fact that the aerodynamic lag effects due to the shed wake become larger with increasing Mach number. The coefficients A_i and b_i can be derived from the aerodynamic response due to harmonic motion. Mazelsky [18, 19] derived exponential forms of the indicial response using theoretical results for the lift on an oscillating airfoil in subsonic compressible flow. Drischler [20] applied the same approach to find exponential approximations for the indicial lift obtained during the penetration of a sharp edge gust, which is also known to be proportional to the circulation obtained during indicial airfoil motion. More recently, the author [21] has obtained an optimized $N = 2$ exponential approximation for ϕ_α^c in the form of Eq. 31 using experimental measurements in the frequency domain at Mach numbers up to 0.8, where $A_1 = 0.918$, $b_1 = 0.366$, $A_2 = 0.082$, and $b_2 = 0.102$.

We may note further that analogous to the incompressible case, in linearized subsonic flow the circulatory lift lag is an intrinsic function of the fluid and does not depend on the airfoil boundary conditions. This result was first examined in some detail by Mazelsky [19, 22] who used numerical results for the unsteady lift and moment response in the frequency domain to extract the separate indicial responses due to angle of attack and pitch rate by means of reciprocal relationships. It was shown that for a pitch rate imposed about the 3/4–chord, a nonimpulsive and finite time-dependent lift exists at $S = 0$ but approaches zero in a few semi-chord lengths of airfoil travel. This lift is entirely of noncirculatory origin, and is consistent with the incompressible result which shows that for a pitch rate imposed about the 3/4–chord, no circulatory lift is produced. In view of the foregoing, it immediately becomes clear that we may write

$$\phi_\alpha^c(S,M) = \phi_q^c(S,M,a) = \phi_\delta^c(S,M,e) = \phi_{\dot\delta}^c(S,M,e) \tag{32}$$

for linearized subsonic compressible flow as well as incompressible flow without any loss of rigor.

During the time between the initial noncirculatory dominated loading until the final circulatory dominated loading is obtained, the flow adjustments are very complex and involves the creation of circulation as well as the propagation and reflection of wave-like pressure disturbances. Mazelsky [23] showed that the noncirculatory lift in subsonic compressible flow decays very rapidly from the initial piston theory values. It has been shown previously [17, 21], that for practical calculations the noncirculatory lift decay for indicial airfoil motion can be closely approximated by exponential functions of the form

$$\Delta C_{L_\alpha}^i(S,M) = \frac{4}{M}\phi_\alpha^i(S,M)\Delta\alpha = \frac{4}{M}\exp\left(\frac{-S}{T_\alpha'(M)}\right)\Delta\alpha \tag{33}$$

$$\Delta C_q^i(S,M,a) = \frac{2(1-2a)}{M}\phi_q^i(S,M,e)\Delta q = -\frac{2a}{M}\exp\left(\frac{-S}{T_q'(M,e)}\right)\Delta q \tag{34}$$

Similarly, for indicial flap motion we will assume (and later justify) exponential decays of the form

$$\Delta C_{L_\delta}^i(S,M,e) = \frac{2(1-e)}{M}\phi_\delta^i(S,M,e)\Delta\delta = \frac{2(1-e)}{M}\exp\left(\frac{-S}{T_\delta'(M,e)}\right)\Delta\delta \tag{35}$$

$$\Delta C_{L_{\dot\delta}}^i(S,M,e) = \frac{(1-e)^2}{2M}\phi_{\dot\delta}^i(S,M,e)\frac{\Delta\dot\delta c}{V} = \frac{(1-e)^2}{2M}\exp\left(\frac{-S}{T_{\dot\delta}'(M,e)}\right)\frac{\Delta\dot\delta c}{V} \tag{36}$$

where $T_\alpha'(M)$, $T_q'(M)$, $T_\delta'(M)$ and $T_{\dot\delta}'(M)$ are all Mach number dependent decay rates or time constants. A final problem then, is to obtain values for these noncirculatory time constants. Note that their proper evaluation critically defines the behavior of the indicial responses at small values of time.

These time constants can be evaluated with the aid of exact solutions for the indicial response, which exist for limited values of time after the perturbation is applied. Lomax et al. [24] and Lomax [25] obtained theoretical results using a form of the wave–equation for the indicial responses due to step changes in airfoil angle of attack and pitch rate. The mathematical calculations are somewhat complex, and solutions can be obtained only for a short period of time after the start of the motion (less than one semi-chord length of airfoil travel), but this is still sufficient to define the initial behavior of the indicial response.

The exact solution for the chordwise pressure on an airfoil undergoing a unit step change in angle of attack is

$$\Delta C_p(x,t_1) = \Re\left\{\frac{8}{\pi(1+M)}\sqrt{\frac{t_1-x}{Mt_1+x}} + \frac{4}{\pi M}\left[\cos^{-1}\left(\frac{t_1(1+M)-2(c-x)}{t_1(1-M)}\right) - \cos^{-1}\left(\frac{2x-t_1(1-M)}{t_1(1+M)}\right)\right]\right\} \tag{37}$$

for the period $0 \le t_1 \le c/(1+M)$, where $\Re$ refers to the real part, and x is measured from the leading edge. The resulting lift on the airfoil can be obtained from

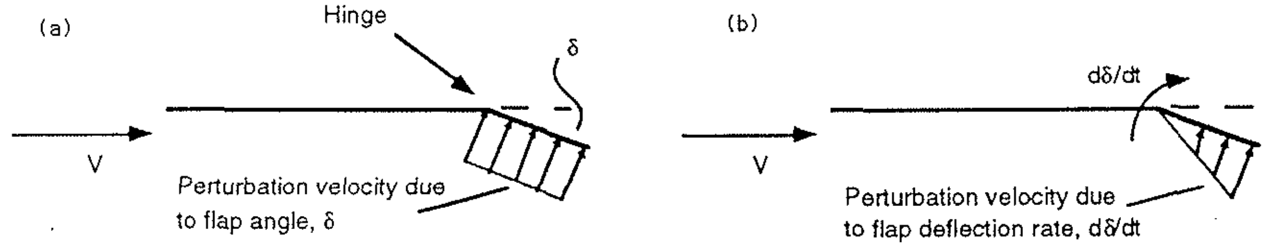

Figure 2: Perturbation velocity due to (a) flap angle, (b) flap rate

$$C_L(t_1) = \int_{-Mt_1}^{c-Mt_1} \Delta C_p(x,t_1)dx \tag{38}$$

and the result can be transformed to the S domain by making use of the fact that $S = 2Mt_1$.

The corresponding indicial responses due to the impulsive motion of a trailing–edge flap can be obtained using Eq. 37, with the aid of the aerodynamic reciprocity relations described by Flax [26], and Heaslet and Spreiter [27]. As long as one is interested in the total lift and moment, it appears that this approach furnishes the only rigorous way of treating the indicial flap problem exactly. However, the result has not appeared previously in the literature,

Consider first, the indicial lift due to flap deflection angle, δ, which produces a uniform perturbation velocity over the flap, as shown in Fig. 2(a). It can be shown by the aerodynamic reciprocal theorems that the *lift in steady or indicial motion per unit angle of flap deflection is equal to the lift per unit angle of attack on the corresponding portion of a flat plate airfoil moving in the reverse direction.* Consider a flapped portion of one airfoil deflected at an angle δ, and the remainder of the airfoil is a flat plate with its surface parallel to the free-stream. Let a second airfoil be a flat plate airfoil at angle of attack α, so that

$$\alpha_1 = \begin{cases} \delta & \text{on the flap} \\ 0 & \text{elsewhere} \end{cases} \qquad \alpha_2 = \text{const.} \tag{39}$$

The reciprocal theorem gives

$$\frac{C_{L_1}(t_1)}{\delta} = \int_{flap} \left(\frac{\Delta C_{p_2}(x_2/c, t_1)}{\alpha_2}\right) d\left(\frac{x_2}{c}\right) \tag{40}$$

where ΔC_p is given by Eq. 37. It can be shown by integration that in the short time interval $0 \leq S \leq M(1-e)/(1+M)$ the indicial lift due to the flap deflection angle is given exactly by

$$\Delta C_{L_\delta}(S) = \frac{2(1-e)}{M}\left[1 - \frac{(1-M)S}{2M(1-e)}\right]\Delta\delta \tag{41}$$

A similar approach can be used to find the initial behavior of the indicial response due to flap rate $\dot{\delta}$ about the hinge. The local perturbation velocity due to this motion is linear, as shown in Fig. 2(b). By means of the reciprocal relations, we can show that *the lift on one airfoil due to flap rate about the hinge is equal to the integral over the airfoil of the product of the perturbation in local angle of attack induced by the flap rate motion and the loading per unit angle of attack at the corresponding point of a second airfoil comprising a flat plate moving in the reverse direction.* Therefore we have

$$\frac{C_{L_1}(t_1)}{\dot{\delta}c/V} = \int_{flap}\left(\frac{\Delta C_{p_2}(x_2/c, t_1)}{\alpha_2}\right)\left(\left(\frac{1-e}{2}\right) - \frac{x_2}{c}\right) d\left(\frac{x_2}{c}\right) \tag{42}$$

In the short time interval $0 \leq S \leq M(1-e)/(1+M)$, it can be shown by integration that the indicial lift on the airfoil due to flap rate varies as

$$\Delta C_{L_{\dot{\delta}}}(S) = \frac{1}{2M}\left[(1-e)^2 - \frac{(1-M)(1-e)S}{M} + \frac{(2-M)S^2}{2M}\right]\frac{\Delta\dot{\delta}c}{V} \tag{43}$$

The reciprocal theorems can also be used to obtain results for the indicial pitching moments, and the general procedure is closely analogous to that described above. Also, results can be obtained for leading–edge flap deflections.

Typical results for the indicial lift due impulsive flap delection are shown in Fig. 3 for $M = 0.5$. Note that these loads are quite different to the incompressible result for indicial flap motion which exhibit an infinite pulse at $S = 0$, and thereafter build progressively from one-half of their final value (c.f. Wagner function). Note that the 100% flap case corresponds to the rigid airfoil pitching about its leading edge ($e = -1$).

From these exact results for the indicial response in subsonic flow, the time constants for the noncirculatory lift decay in Eqs. 33-36 can be approximated by equating the sum of the time derivatives of the assumed exponential forms of the noncirculatory and circulatory lift response at time zero ($S = 0$) to the corresponding time derivative of the exact solutions, i.e.,

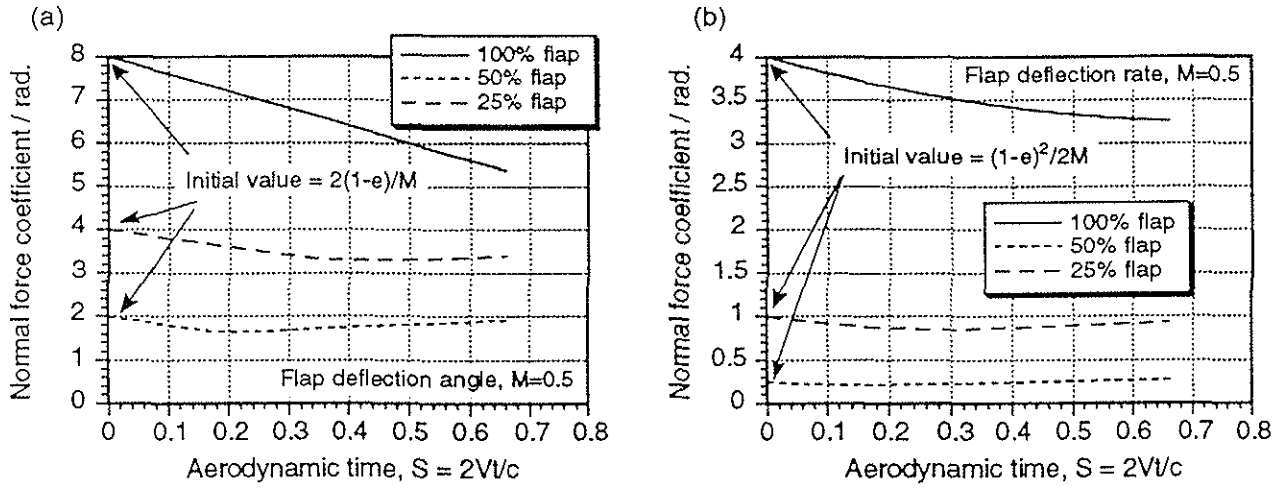

Figure 3: Indicial lift computed using exact linear theory at $M = 0.5$ due to (a) flap deflection, and (b) flap rate

$$\underbrace{\left.\frac{dC_L}{dS}\right|_{S=0}}_{\text{exact}} = \underbrace{\left.\frac{dC_L^c}{dS}\right|_{S=0}}_{\textit{circ.}} + \underbrace{\left.\frac{dC_L^i}{dS}\right|_{S=0}}_{\textit{non-circ}} \tag{44}$$

Based on this approach, which is outlined for the airfoil angle of attack and pitch rate terms (i.e., the T_α and T_q terms) in [21], the noncirculatory time constants for the flap can be expressed in terms of the coefficients of the approximating circulatory response as

$$T_\delta(M,e) = \kappa_\delta\left(\frac{c}{2V}\right)T'_\delta = \kappa_\delta(1-e)\left[(1-M) + F_{10}\beta^{-1}M^2\sum_{i=1}^{2}A_i b_i\right]^{-1}\left(\frac{c}{a_s}\right) = K_\delta(M,e)\,T_i \tag{45}$$

$$T_{\dot\delta}(M,e) = \kappa_{\dot\delta}\left(\frac{c}{2V}\right)T'_{\dot\delta} = \kappa_{\dot\delta}\frac{(1-e)^2}{2}\left[(1-M)(1-e) + F_{11}\pi^{-1}\beta^2M^2\sum_{i=1}^{2}A_i b_i\right]^{-1}\left(\frac{c}{a_s}\right) = K_{\dot\delta}(M,e)\,T_i \tag{46}$$

Note also that in the above representation, the actual values for the circulatory coefficients A_i and b_i are nonessential since the noncirculatory time constants are always adjusted to give the correct initial behavior of the total indicial lift response given by the exact linear theory. The constants κ_δ, and $\kappa_{\dot\delta}$ are assumed here to be empirical parameters in the ranges $0.70 \le \kappa_\delta, \kappa_{\dot\delta} \le 1.0$. These constants are necessary to modify the initial behavior of the indicial lift decay, which on the basis of correlation studies with test data has been found justified because of additional physical effects such as airfoil thickness, loss of flap effectiveness and minor viscous effects. These effects, of course, are not accounted for in the linear theory. *

The results obtained from this process are shown for the indicial lift due to angle of attack and pitch rate at $M = 0.5$ in Figs. 4 and 5, respectively. In each case, the first graph shows the results at small values of time, and the second graph shows the subsequent build–up of the circulatory lift at greater values of time. Note the excellent agreement between the exponential approximations and the exact theory for smaller values of time. At later time, the solutions begin to differ because of the fact that the present circulatory solution has been *partially derived from experimental results and not only the linear theory.*

Consider now the lift response due to arbitrary flap deflection in subsonic compressible flow. Since the circulatory part of the indicial response does not depend on the mode of forcing, the flap deflection angle and the pitch rate about the hinge can be combined into a single term, i.e., δ_{qs}, as shown previously for the incompressible case. The state-space equivalent of

$$\delta_{qs}(0)\phi_\delta^c(S,M) + \int_0^S \frac{d\delta_{qs}}{d\sigma}\phi_\delta^c(S-\sigma,M)\,d\sigma \tag{47}$$

can be written in controllable canonical form as

*For the present article we will assume $\kappa_\delta = \kappa_{\dot\delta} = 1$.

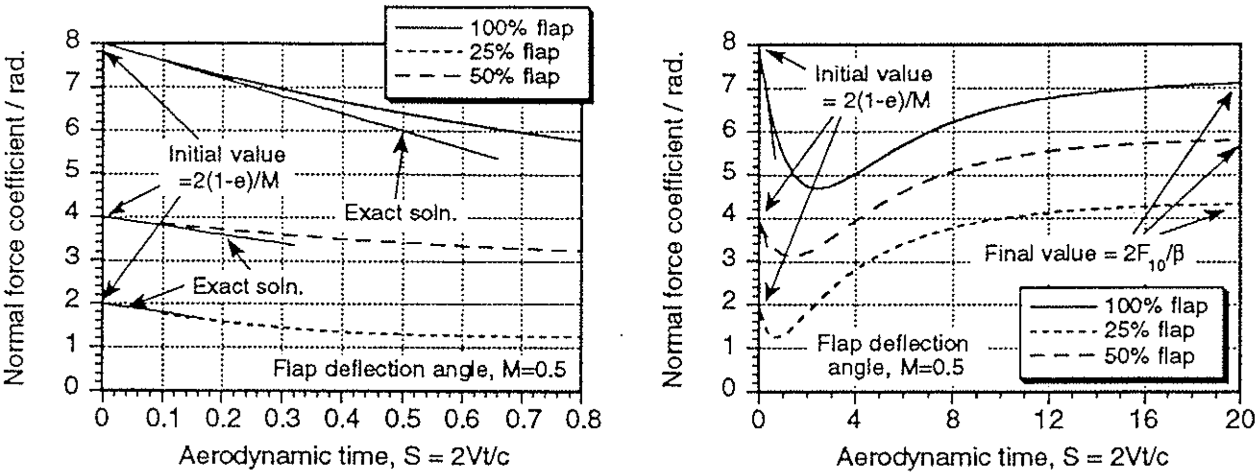

Figure 4: Indicial lift due to flap deflection at $M = 0.5$

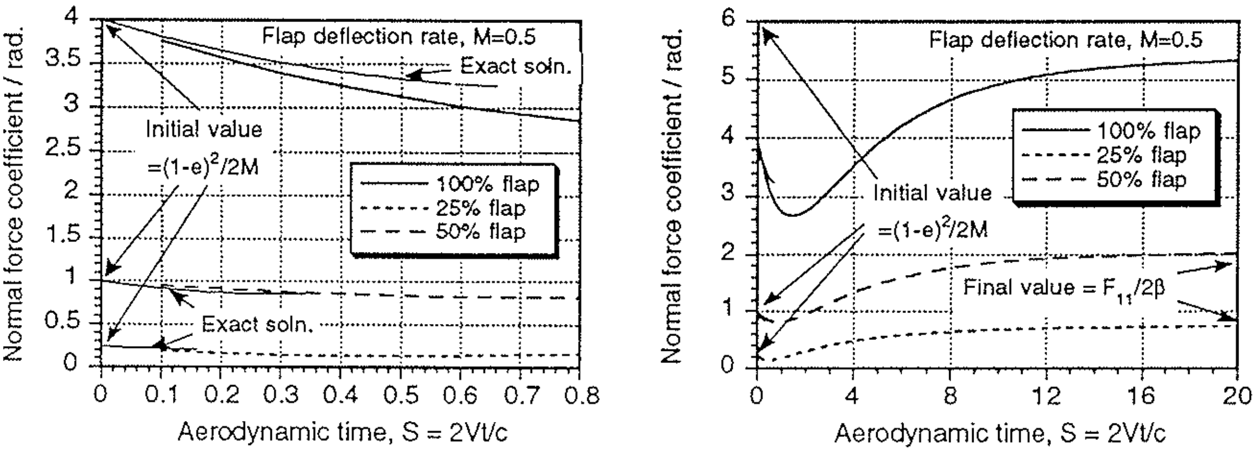

Figure 5: Indicial lift due to flap rate at $M = 0.5$

$$\begin{bmatrix} \dot{z}_1(t) \\ \dot{z}_2(t) \end{bmatrix} = \begin{bmatrix} 0 & 1 \\ -b_1 b_2 (2V/c)^2 \beta^4 & -(b_1 + b_2)(2V/c)\beta^2 \end{bmatrix} \begin{bmatrix} z_1(t) \\ z_2(t) \end{bmatrix} + \begin{bmatrix} 0 \\ 1 \end{bmatrix} \delta_{qs}(t) \tag{48}$$

with the output equation for the circulatory part of the unsteady lift due to the flap

$$C_L^c(t) = \frac{2\pi}{\beta} \left[\, (b_1 b_2)(2V/c)^2 \beta^4 \quad (A_1 b_1 + A_2 b_2)(2V/c)\beta^2 \,\right] \begin{bmatrix} z_1(t) \\ z_2(t) \end{bmatrix} \tag{49}$$

where A_1, b_1 etc. are for subsonic flow as given by Eq. 31. While the other circulatory parts due to airfoil motion can also be combined into the above two state equations, as for the incompressible case, the noncirculatory lift components have a time-history effect in subsonic flow and must be considered separately. The noncirculatory part of the unsteady lift due to arbitrary flap deflection, $\delta(t)$, can be written as

$$\dot{z}_3(t) = \delta(t) - \frac{1}{K_\delta T_i} z_3(t) \qquad C_{L_\delta}^i(t) = \frac{2(1-e)}{M} \dot{z}_3(t) \tag{50}$$

Similarly, the noncirculatory lift due to flap rate about the hinge, $\dot{\delta}(t)$, can be written as

$$\dot{z}_4(t) = \frac{(1-e)^2}{2} \frac{\dot{\delta}(t) c}{V} - \frac{1}{K_{\dot{\delta}} T_i} z_4(t) \qquad C_{L_{\dot{\delta}}}^i(t) = \frac{(1-e)^2}{4M} \frac{c}{V} \dot{z}_4(t) \tag{51}$$

The remainder of the unsteady loads due to airfoil motion and due to encounters with an arbitrary gust field can be obtained in state–space form following the procedures outlined in Refs. [21] and [28], and can be easily appended to the equations describing the flap.

RESULTS AND DISCUSSION

From the state equations given above, the response to a particular harmonic motion of the flap can be derived in closed form. While the algebraic manipulation is somewhat lengthy, it can be shown that for a prescribed harmonic forcing explicit expressions can be obtained for the lift on the airfoil as a function of flap frequency. This provides an independent check of the aerodynamic approximations independently of any numerical integration scheme.

Typical results for a oscillatory flap motion are shown in Fig. 6. The flap is 25% of the airfoil chord, i.e., $e = 0.5$. The results are presented as the first harmonic lift amplitude and phase angle versus the flap reduced frequency for various Mach numbers, and are compared with the incompressible case. It is clear that the effects of Mach number on the lift response are relatively large. In the limit as $k \rightarrow 0$, the lift amplitude is given by the usual linearized steady flow value and the phase angle is zero. As k increases, the lift amplitude decreases progressively in the range up to $k = 1$. The corresponding phase angle initially exhibits a lag, which is due to the effects of the shed wake vorticity (circulatory component of response). For values of k greater than about 0.4, the phase lag reaches a maximum and thereafter becomes progressively less, ultimately becoming a phase lead at $k = 1$ at the lower Mach numbers. This result is due to the increasing influence of the noncirculatory terms at higher reduced frequencies. The increasing phase lag effects in the lift response with increasing Mach number are particularly worthy of note. Note also the differences in the phase of the response compared to the incompressible case at higher reduced frequencies, even at low free–stream Mach numbers. Physically, this is because pressure perturbations propagate through the flow at the local speed of sound, and at higher flap frequencies the disturbances do not propagate sufficiently quickly relative to the flap motion for the flow to be considered as incompressible.

Further results are shown in Fig. 7, which shows the frequency response for different sizes of trailing–edge flap at $M = 0.5$. The same general trends shown previously are apparent here. However, note that with the slightly larger flap ($e = 0.75$), the phase lead becomes apparent at a much lower reduced frequency. Conversely, with a smaller trailing–edge flap, the lift response is dominated by the circulatory response.

In order to evaluate the theory using direct time integration, the state equations were integrated with respect to time using a standard ordinary differential equation solver. For these particular calculations, the integration was performed using the ODE solver DE/STEP given in Ref.[29], which is a general purpose Adams-Bashforth ODE solver with variable step size and variable order. Typical results for the incompressible case are shown in Fig. 8, both versus time and versus flap angle. Again, for all calculations the trailing–edge flap comprises 25% of chord, i.e., $e = 0.5$. When plotted versus time, the lift is sinusoidal of a somewhat lower amplitude and either leads or lags the flap forcing depending on the magnitude of the reduced frequency. When plotted versus flap angle, the lift exhibits a characteristic elliptical loop, essentially similar to that obtained on an airfoil oscillating in angle of attack. As the frequency increases, the slope of the major axis of the loop becomes less, corresponding to the reduction in lift amplitude shown in Fig. 6. Note that the loop is circumvented in a counterclockwise direction at low reduced frequencies, and develops into a clockwise loop (phase lead) at higher frequencies as the noncirculatory terms begin to dominate. Qualitatively (but not quantitatively) similar results are obtained at all Mach numbers.

As an application that exercises the full range of the unsteady aerodynamic model, including the trailing–edge flap, consider a transient type problem such as an airfoil-vortex interaction. On a helicopter rotor there are a large number of vortical disturbances that lie in proximity to the blades. This is especially the case for the advancing side of the rotor when the helicopter is descending, where the blades may repeatedly encounter a number of close and almost parallel interactions with wake vortices. This blade vortex interaction (BVI) problem is a highly unsteady phenomenon, and is a significant source of higher harmonic rotor airloads, as well as obtrusive noise. Recent civil and military noise requirements have dictated a significant reduction in BVI noise. This objective is difficult to achieve, but it may be possible by the use of active trailing-edge flaps, to

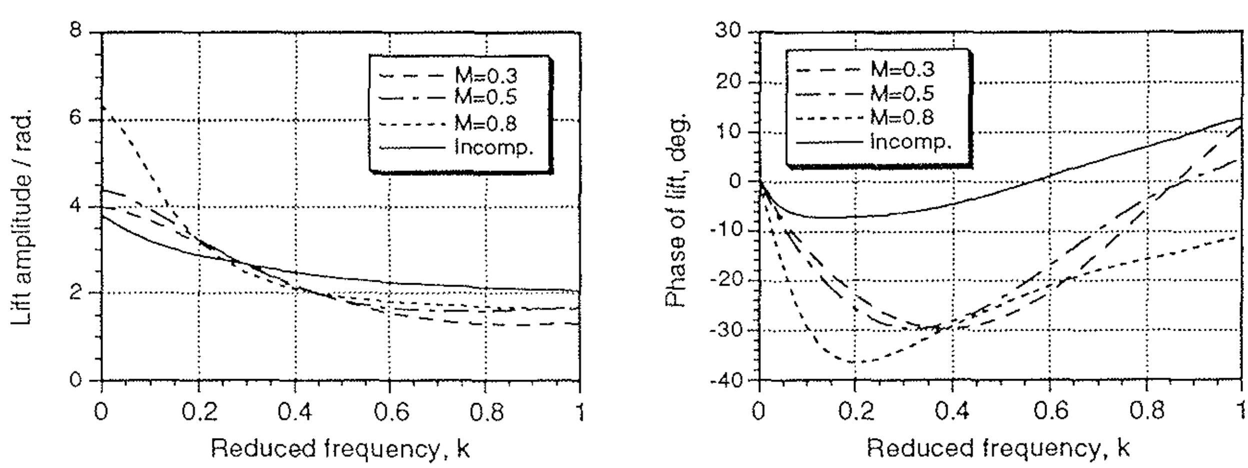

Figure 6: Frequency response due to a harmonic flap oscillation, $\delta = 5^\circ \sin \omega t, e = 0.5$

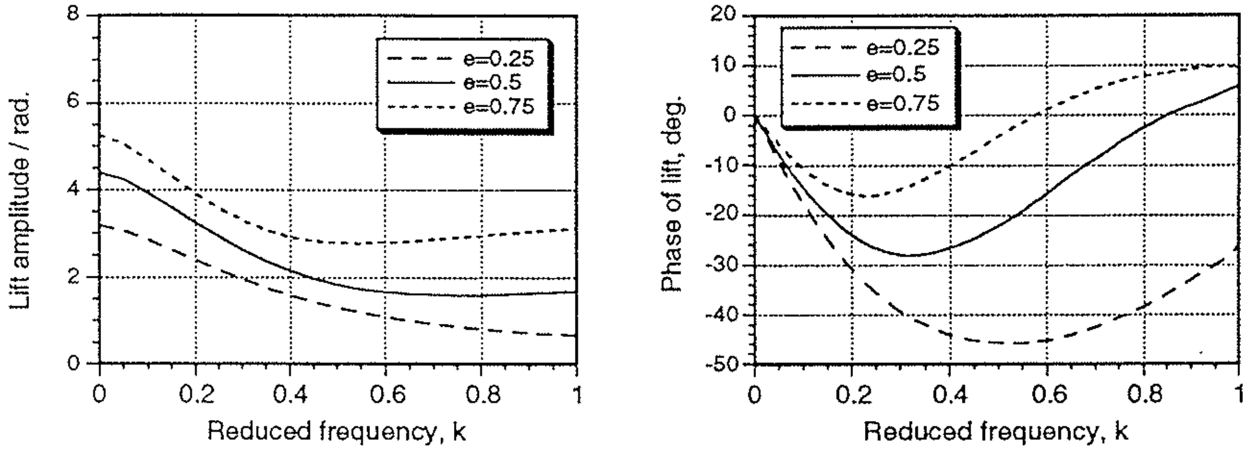

Figure 7: Frequency response due to a harmonic flap oscillation, $\delta = 5° \sin \omega t, M = 0.5$

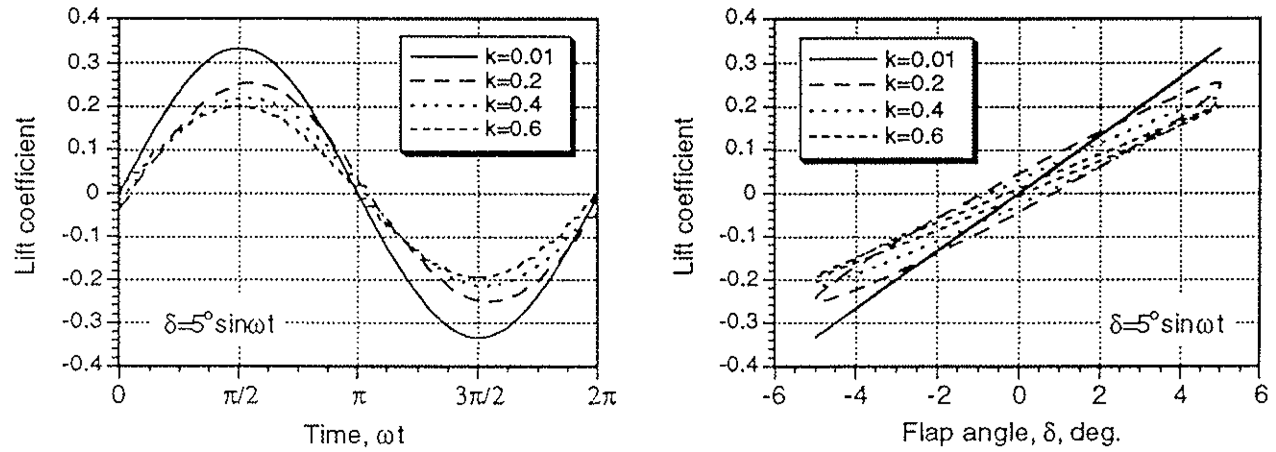

Figure 8: Unsteady lift for a harmonic flap oscillation in incompressible flow

either help modify the unsteady loads during BVI by means of appropriate flap deflection [30, 31], and/or by using the flap to locally change the rotor flapping response thereby increasing the vortex miss–distance. In either case, another fundamental aspect of the problem is the construction of a suitable feedback system.

The BVI problem was studied for incompressible flow by Sears[32] using the sharp-edge gust entry lift function (Küssner function) along with Duhamel superposition. For subsonic compressible flow, there have been many significant theoretical contributions to the BVI problem, e.g., Refs. [33] and [34] and the references contain therein. However, since transonic effects are often present, there has been considerably more progress in understanding this BVI problem in light of recent developments in CFD, see for example Refs. [35] and [36]. Consider two simple examples of a BVI encounter, with and without the application of a trailing edge flap during the encounter. The convecting vortex is of circulation strength $\hat{\Gamma} = \Gamma/cV = 0.2$ and has an irrotational core. The vortex travels at a steady velocity at 0.26 chords below the airfoil. This is a standard case that has received considerable attention in the literature - see Ref. [36]. While passing the blade (airfoil) at this predetermined distance, the vortex produces a downwash while upstream of the airfoil that changes to an upwash as it moves downstream. This situation causes a dynamically changing angle of attack, and so rapidly changing aerodynamic loads are produced on the airfoil.

The downwash variation induced by the passing vortex was used in conjunction with the aerodynamic state equations to solve for the unsteady lift. The integration of the state equations was, again, performed using the Adams-Bashforth ODE solver DE/STEP. Fig. 9 shows results for the reference case, which essentially demonstrate the effects of compressibility on this problem. Results from an Euler code calculation are also shown, which help to validate the more approximate solution used here. Note that compressibility effects produce an attenuation in the peak–to–peak values of the lift. This is despite a higher overall lift curve slope at the higher Mach numbers, which based on incompressible (but unsteady) assumptions will always produce a higher overall peak–to–peak lift. It is significant that when compressibility effects are properly introduced through the form of the indicial (gust) function (Eq. 31), the opposite effect is obtained, and the peak–to–peak lift during the interaction is reduced. This is mainly because in subsonic compressible flow the unsteady airloads take much longer to readjust to the rapidly changing effective angle of attack induced by the vortex. Similar results of the effects of compressibility for this type of BVI problem are shown in the work of Adamczyk [37].

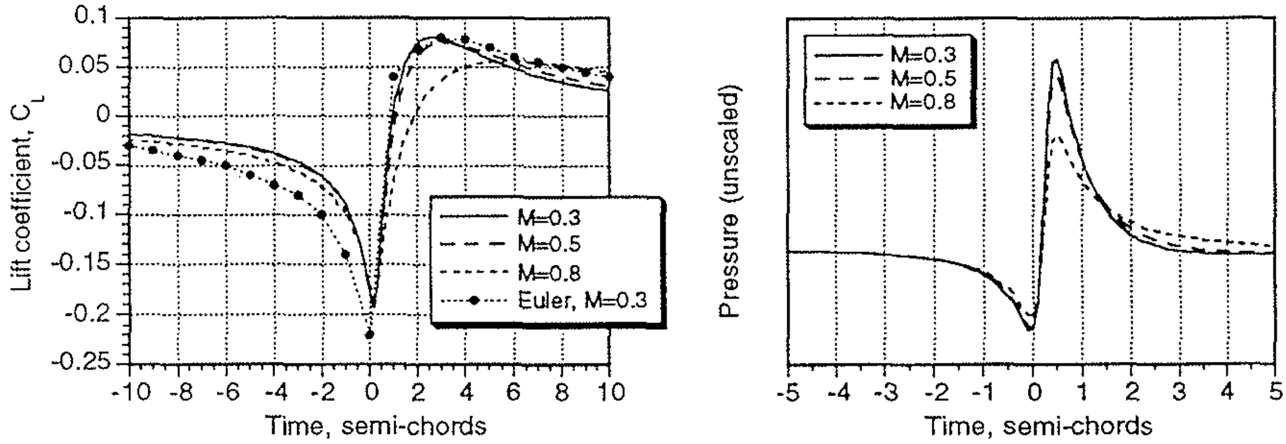

Figure 9: Unsteady lift and noise produced by a BVI at various Mach numbers

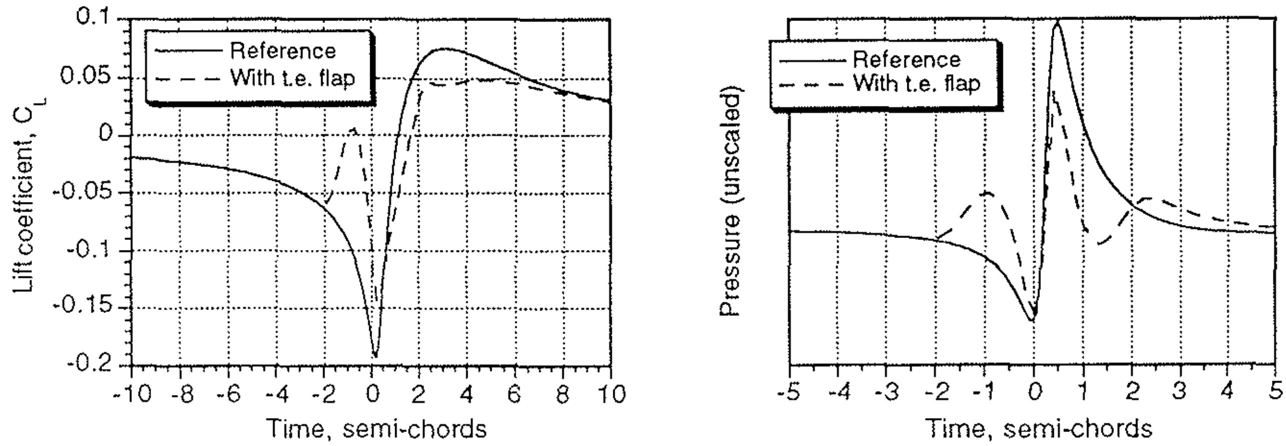

Figure 10: Unsteady lift and noise produced by BVI with and without unsteady flap deflection at $M = 0.5$

Fig. 9 also shows the corresponding acoustic pressure. On a helicopter rotor, the acoustic pressure (or noise) propagated to an observer from such a blade-vortex encounter is related (in the compact source limit) to the time rate–of–change of the aerodynamic lift. The far field acoustic pressure is immediately available in the present form of solution since the time derivatives of the aerodynamic states are already computed by the ODE solver. Note that the acoustic pressure in Fig. 9 is unscaled since the distance or path of a reference point in the far–field is not specified.

Fig. 10 shows results for the unsteady lift and corresponding acoustic pressure obtained during a BVI encounter, but with the rapid application of a trailing–edge flap during the interaction process. For simplicity, a prescribed flap displacement is considered in the form of a doublet with displacement amplitude 2.5 degrees applied over a period of 5 semi–chords of airfoil travel. † The general objective is to use the flap displacement to alter the time rate–of–change of the aerodynamic loads, and therefore reduce/modify the acoustic signature due to the BVI phenomenon. It is unnecessary (or even undesirable) to completely destroy the lift during this process, since on a rotor this may adversely alter the blade loads and rotor flapping response over other parts of the rotor disk. It should also be remembered that the motion of the flap introduces its own unsteady lift response due to flap displacements and rate terms, and so the incremental change in lift produced by the flap relative to the reference case does not necessarily mimic the doublet input either in amplitude or in phase. Nevertheless, it can be seen from Fig. 10 that there is some overall reduction in the peak–to–peak lift through the application of the flap.

Fig. 10 also shows that the influence of the vortex affects the lift relatively far upstream, but the acoustic signature is affected only when the vortex is about two chord lengths upstream and downstream of the airfoil. The transient nature of the pressure spike obtained is essentially one source of helicopter rotor noise that has become well known as "blade slap." It is clear from the example presented that the imposed flap motion certainly helps attenuate the peak–to–peak noise during the interaction, however, in no way should this result be considered optimum. In fact, the abruptness of this phenomenon and the necessity of modifying the time

†In practice, the actual flap displacement will be controlled by a closed–loop feedback system.

rate–of–change of the airloads (as opposed to the airloads directly) posses special problems in the design of a feedback controller for active noise reduction on rotors due trailing–edge flap deflections.

CONCLUDING REMARKS

This article has addressed the development of a practical method of computing the unsteady lift due to arbitrary flap deflection in a subsonic compressible flow. The motivation has partly stemmed from a requirement to compute unsteady loads and acoustics within the confines of a comprehensive rotor analysis due to the active deflection of part–span trailing–edge flaps on the blades. In the present article, exact solutions for indicial flap displacement and flap rate were obtained for small values of time from the indicial airfoil case in conjunction with aerodynamic reciprocal relations. The results were then generalized to later values of time in terms of exponential approximations. These approximations were finally used to obtain state equation for the lift response due to arbitrary flap motions. By an extension of the present approach, the pitching moment can also be derived.

Results have been presented that show the general effects of time–dependent trailing–edge flap motions on the unsteady lift response. For oscillatory flap forcing, the unsteady lift lags the flap motion at low flap reduced frequencies and begins to lead the flap forcing at higher frequencies. The effects of Mach number on the aerodynamic response were shown to be significant, and essentially manifest themselves as larger aerodynamic lags at higher Mach numbers. The differences between classical incompressible theory and compressible theory (albeit partial based on experiment) were sufficiently large to render the classical theory insufficient for the combination of Mach numbers and reduced frequencies likely to be found on rotor blades with actively controlled trailing–edge flaps. Finally, an application of the method to a simulated blade-vortex encounter were made. It was shown that the unsteady lift and sound pressure produced by such interactions could be altered beneficially by the application of appropriate flap displacements during the encounter. However, bearing in mind the three–dimensional compexity of the BVI phenomenon in an actual rotor environment, the active control of rotor loads and/or noise by means of trailing–edge flaps must remain the subject of further investigation.

ACKNOWLEDGEMENTS - This work was partially supported by the U.S. Army Research Office under contract DAAL03-92-G-0121, "Smart Structures Technology: Innovations & Applications to Rotorcraft Systems," Dr. Garry Anderson was the technical monitor.

REFERENCES

[1] Edwards, J.W., "Flight Test Results of an Active Flutter Suppression System," *Journal of Aircraft*, Vol. 20, No. 3, pp. 267-274, March 1983.

[2] Millott, T.A., Friedmann, P.P., "Vibration Reduction in Helicopter Rotors using an Active Control Surface Located on the Blade," AIAA Paper 92-2451-CP, Proceedings of the *AIAA/ASME/ASCE/AHS/ASC Structures, Stuctural Dynamics and Materials Conference*, Dallas, Texas, April 13-15, 1992.

[3] Chen, P.C., Samak, D.K., Chopra, I., "Development of an Intelligent Rotor," Proceedings of the *4th Workshop on Dynamics and Aeroelasticity Modelling of Rotorcraft Systems*, College Park, MD, Nov. 20, 1991.

[4] van der Wall, B., Leishman, J.G., "The Influence of Variable Flow Velocity on Unsteady Airfoil Behavior," Paper No. 81, *Proceedings of the 18th European Rotorcraft Forum*, Avignon, France, Sept. 15-18, 1992.

[5] Küssner, H.G., Schwartz, L., "The Oscillating Wing with Aerodynamically Balanced Elevator," NACA Translation TM 991, 1941.

[6] Theodorsen, T., "General Theory of Aerodynamic Instability and the Mechanism of Flutter," NACA Report 496, 1935.

[7] Theodorsen, T., Garrick, I.E., "Nonstationary Flow about a Wing-Aileron-Tab Combination, Including Aerodynamic Balance, NACA Report 736, 1942.

[8] Von Karman, Th., Sears, W.R., "Airfoil Theory for Non-Uniform Motion," *Journal of the Aeronautical Sciences*, Vol. 5, No. 10, pp. 379-390, Aug. 1938.

[9] Sears, W.R., "Operational Methods in the Theory of Airfoils in Nonuniform Motion," *Journal of the Franklin Institute*, Vol. 230, pp. 95-111, July 1940.

[10] Bisplinghoff, R.L., Ashley H. and Halfman, R.L., *Aeroelasticity*, Addison-Wesley, 1955.

[11] Jones, R.T., "The Unsteady Lift of a Wing of Finite Aspect Ratio," NACA Report 681, 1940.

[12] Jones, W.P., "Aerodynamic Forces on Wings in Non-Uniform Motion," ARC R&M 2117, 1945.

[13] Peterson, L.D., Crowley, E.F., "Improved Exponential Time Series Approximation of Unsteady Aerodynamic Operators," *Journal of Aircraft*, Vol. 25, No. 2, pp. 121-127, Feb. 1988.

[14] Eversman, W., Tewari, A., "Modified Exponential Series Approximation for the Theodorsen Function," *Journal of Aircraft*, Vol. 28, No. 9, pp. 553-557, Sept. 1991.

[15] Turner, M.J., Rabinowitz, S., "Aerodynamic Coefficients for an Oscillating Airfoil with Hinged Flap, with Tables for a Mach Number of 0.7," NACA TN 2213, 1950.

[16] Beddoes, T.S., "Practical Computation of Unsteady Lift," *Proceedings of the 7th. European Rotorcraft Forum*, Sept. 1982. See also *Vertica* Vol. 8, No. 1, pp. 55-71, 1984.

[17] Leishman, J.G., "Validation of Approximate Indicial Aerodynamic Functions for Two-Dimensional Flow," *Journal of Aircraft*, Vol. 25, No. 10, pp. 914-922, Oct. 1988.

[18] Mazelsky, B., "Numerical Determination of Indicial Lift of a Two-Dimensional Sinking Airfoil at Subsonic Mach Numbers from Oscillatory Lift Coefficients with Calculations for Mach Number of 0.7," NACA TN 2562, 1951.

[19] Mazelsky, B., "Determination of Indicial Lift and Moment of a Two-Dimensional Pitching Airfoil at Subsonic Mach Numbers from Oscillatory Coefficients with Numerical Calculations for a Mach Number of 0.7," NACA TN 2613, Feb. 1952.

[20] Drishler, J.A., "Calculation and Compilation of the Unsteady Lift Functions for a Rigid Wing Subjected to Sinusoidal Gusts and to Sinking Oscillations," NACA TN 3748, October 1956.

[21] Leishman. J.G., "Indicial Lift Approximations for Two-Dimensional Subsonic Flow as Obtained from Oscillatory Measurements," To appear in the Journal of Aircraft, July/Aug. 1992.

[22] Mazelsky, B., Drischler, J.A., "Numerical Determination of Indicial Lift and Moment Functions of a Two-Dimensional Sinking and Pitching Airfoil at Mach Numbers 0.5 and 0.6," NACA TN 2739, 1952.

[23] Mazelsky, B., "On the Noncirculatory Flow About a Two-Dimensional Airfoil at Subsonic Speeds," *Journal of the Acronautical Sciences*, Vol. 19, Vol. 12, pp. 848-849, Dec. 1952.

[24] Lomax, H., Heaslet, M.A., Fuller, F.B., and Sluder, L., "Two and Three Dimensional Unsteady Lift Problems in High Speed Flight," NACA Report 1077, 1952.

[25] Lomax, H., "Indicial Aerodynamics," *AGARD Manual of Aeroelasticity*, Part II, Chapter 6, Nov. 1960.

[26] Flax, A.H., "Reverse-Flow and Variational Theorems for Lifting Surfaces in Nonstationary Compressible Flow," *Journal of the Aeronautical Sciences*, Vol. 20, No. 2, pp. 120-126, Feb. 1952.

[27] Heaslet, M.A., Spreiter, J.R., "Recipocity Relations in Aerodynamics," NACA Report 1119, 1953.

[28] Leishman, J.G., Nugyen, K.Q., "A State-Space Representation of Unsteady Aerodynamic Behavior," *AIAA Journal*, Vol. 28, No. 5, pp. 836-845, May 1990.

[29] Shampine, L.F., Gordon, M.K., *Computer Solution of Ordinary Differential Equations - The Initial Value Problem*, W.H. Freeman and Co., San Francisco, 1975.

[30] McCroskey, W.J., "The Effects of Gusts on the Fluctuating Airloads of Airfoils in Transonic Flow," *Journal of Aircraft*, Vol. 22, No. 3, pp. 236-243, March 1985.

[31] Hassan, A.A., Sankar, L.N., Tadghighi, H., "Effects of Leading and Trailing-Edge Flaps on the Aerodynamics of Airfoil Vortex Interactions," Proceedings of the AHS Specialists Meeting on Rotorcraft Basic Research, Atlanta, GA, March 25-27, 1991.

[32] Sears, W.R., "Aerodynamics, Noise and the Sonic Boom," *AIAA Journal*, Vol. 7, No.4, pp. 577-586, April 1969.

[33] Widnal, S., "Helicopter Noise due to Blade Vortex Interaction," *Journal of the Acoustical Society of America*, Vol. 50, No. 1, Pt. 2, pp. 345-365, 1971.

[34] Amiet, R.K., "Airfoil Gust Response and the Sound Produced by Airfoil-Vortex Interaction," *Journal of Sound and Vibration*, Vol. 107, No. 3, pp. 487-506, 1986.

[35] McCroskey, W.J., Goorjian, P.M., "Interactions of Airfoils with Gusts and Concentrated Vortices in Unsteady Transonic Flow," AIAA Paper 83-1691, July 1983.

[36] Srinivasan, G.R., McCroskey, W.J., "Numerical Simulations of Unsteady Airfoil Interactions," *Vertica*, Vol. 11, No. 1/2, pp. 3-28, 1987.

[37] Adamczyk, J.J. "Passage of a Swept Airfoil through an Oblique Gust," *Journal of Aircraft*, Vol. 11, No. 5, pp. 281-287, May 1974.